FITTING COSINES: SOME PROCEDURES AND SOME PHYSICAL EXAMPLES*

David R. Brillinger

Technical Report No. 49

October 1985

*Research Supported by National Science Foundation Grant DMS - 8316634

Department of Statistics
University of California
Berkeley, California

David R. Brillinger

FITTING COSINES: SOME PROCEDURES AND SOME PHYSICAL EXAMPLES

ABSTRACT

The paper is concerned with a variety of time series models that in some sense lead to the fitting of a cosine funstion of unknown frequency. Both linear and nonlinear models are considered, including both decaying cosines and sustained ones. The discussion is illustrated with examples from seismology (free oscillations of the Earth), geophysics (the Chandler wobble), nuclear magnetic resonance, laser Doppler velocimetry and oceanography (dispersion). The paper ends by surveying a variety of results developed for specific models by various authors. A variety of open problems are indicated.

"The aim of science is to seek the simplest explanation of complex facts ... seek simplicity and distrust it."

A. N. Whitehead

1. INTRODUCTION

There are a broad variety of natural phenomena that are periodic and that have been studied since early times. Some of these, and their researchers, are: the planets (Kepler), pendulums (Galileo), the violin string (Mersenne), light (Huyghens), sound (Newton) and crystals. Cosines were fit numerically to orbital data as early as 1754 (see Clairaut (1754) and Heideman et al. (1984).) Several arguments may be set down for the genesis of cosines. Linear combinations of cosines provide the general solution of differential equations with constant coefficients - and such equations provide effective descriptions of many phenomena. Cosines and more general periodic functions result from the repeated application of various operators. The input to a system may be periodic, and in consequence the ouput is as well. Finally, the experimental setup may be such that periodically varying data is collected.

A key property of cosines is that they persist under linear time invariant operations. This is formalized in Lemma 2.7.1 of Brillinger (1975), but may be illustrated quickly as follows. Suppose

$$Y(t) = \sum_{u=-\infty}^{\infty} a(u)\, X(t-u) \tag{1}$$

The operation carrying $X(\cdot)$ into $Y(\cdot)$ is linear and time invariant. If $X(t) = \exp\{i\lambda t\}$, then $Y(t) = A(\lambda)\exp\{i\lambda t\}$, with

$$A(\lambda) = \sum_{u} a(u) \exp\{-i\lambda u\} \tag{2}$$

Here, following de Meivre's formula, $\exp\{i\lambda t\} = \cos \lambda t + i \sin \lambda t$ and because of the linearity of the operation (1), the effect of the operation on the cosine function $\cos \lambda t$ may be seen. In the case that λ is real-valued it is referred to as the frequency (in radians per unit time.) Because many naturally occurring operations are, to a good approximation, linear and time invariant the nonentaglement of cosine waves of different frequencies can allow one to look back to the generation process of a phenomenon of interest.

Fourier transforms play essential roles in the study of periodic phenomena and of linear time invariant systems. Definition (2) shows the transfer function, $A(\cdot)$, to be the Fourier transform of the impulse response, $a(\cdot)$. For the model -

$$Y(t) = \rho \cos(\gamma t + \delta) + \varepsilon(t) \tag{3}$$

$t = 0,\pm1,\pm2,\cdots$ with $\varepsilon(\cdot)$ a noise process, the least squares estimate of $\rho \exp\{i\delta\}$ is approximately

$$\frac{2}{T} \sum_{t=0}^{T-1} Y(t) \exp\{-i\gamma t\} \tag{4}$$

when γ is known and the data $Y(t)$, $t=0,\cdots,T-1$ are available. The values

$$\sum_{t=0}^{T-1} Y(t) \exp\{-i2\pi st/T\} \tag{5}$$

$s = 0,\cdots,T-1$ are referred to as the discrete Fourier transform of the data stretch $Y(t)$, $t = 0,\cdots,T-1$. In a variety of circumstances these values may be computed exceedingly rapidly via a fast Fourier transform (FFT) algorithm, Heideman et al. (1984). Astonishingly such an algorithm was known to Gauss in 1805, ibid..

This paper is a mixture of review of existing results, physical examples, models and methods relating to the fitting of cosines to both linear and nonlinear phenomena. The main sections are: Decaying Cosines, Noise Sustained Oscillations, Dispersion and Modes, a Review of Some Particular Results and Some Open Problems.

2. DECAYING COSINES

2.1 Some Conceptualization

Vibratory motion pervades and unifies the physical sciences. A mathematical conceptualization that is consistent with this observation is that a great variety of natural systems may be described by systems of equations of the form

$$\frac{d\underset{\sim}{Y}(t)}{dt} = \underset{\sim}{A}\,\underset{\sim}{Y}(t) + \underset{\sim}{X}(t) \tag{6}$$

with $\underset{\sim}{X}(\cdot)$ vector-valued input and with $\underset{\sim}{Y}(\cdot)$ vector-valued output or perhaps a state vector. In the case that the input is $\underset{\sim}{b}\,\delta(t)$, $\delta(\cdot)$ the Dirac delta, and intitial conditions are $\underset{\sim}{Y}(0-) = \underset{\sim}{0}$, then the general solution of (6) may be written

$$\begin{aligned} \underset{\sim}{Y}(t) &= \exp\{\underset{\sim}{A}t\}\,\underset{\sim}{b} \qquad\qquad t > 0 \\ &= \sum_j \alpha_j \exp\{\mu_j t\}\,\underset{\sim}{u}_j \end{aligned} \tag{7}$$

where μ_j, $\underset{\sim}{u}_j$ are the (assumed distinct) latents of the matrix $\underset{\sim}{A}$. Focussing on any one of the coordinates of $\underset{\sim}{Y}(\cdot)$ then,its motion has the form

$$\sum_{k=1}^{K} \rho_k \exp\{-\sigma_k t\} \cos(\gamma_k t + \delta_k) \tag{8}$$

for $t > 0$, with $-\sigma_k$ and γ_k the real and imaginary parts of one of the μ_j . This has the empirical implication that one is sometimes led to model time series data as the sum of the term (8) and a noise process.

2.2 Free Oscillations of the Earth

After a great earthquake, the whole Earth may oscillate for many days, see for example Bolt (1982, Chapter 6). From these oscillations, or free vibrations, the seismologist infers much about the structure of the Earth. The equations of motion may be written in the form of (6), for the many particles making up the Earth. A great earthquake may be viewed as providing a delta function type input. In consequence a corresponding seismic record may be viewed as having the form

$$Y(t) = \sum_{k=1}^{K} \rho_k \exp\{-\sigma_k t\} \cos(\gamma_k t + \delta_k) + \varepsilon(t) \tag{9}$$

$\varepsilon(\cdot)$ being a noise process. (It is worth noting that K may be greater than 1500 for some events.) The seismologist is particularly interested in estimating the γ_k and σ_k for he is then able to compare these observed values with corresponding values for an Earth model that he has constructed. A traditional procedure for estimating the γ_k in a model such as (9) is to look for the locations of peaks in the periodogram. Specifically, let

$$d_Y^T(\lambda) = \sum_{t=0}^{T-1} Y(t) \exp\{-i\lambda t\} \tag{10}$$

denote the Fourier transform of a stretch of data, then the periodogram is defined as

$$I_{YY}^T(\lambda) = (2\pi T)^{-1} |d_Y^T(\lambda)|^2 \tag{11}$$

It may be expected to show peaks in the neighborhood of the γ_k of (9) with their respective heights depending on the values of the other parameters appearing.

Figure 1 is a record of the Great Chilean earthquake of 22 May 1960 as recorded at Trieste. The tides have been removed from the original displacements measured. Many oscillations are present and it is apparent that these decay. Figure 2 is a graph of the log periodogram,(11), for one frequency interval. It was based on 2548 points with a sampling interval of 2 minutes, (hence a longer time period than that shown in Figure 1.) Many peaks are apparent. To gain some idea of the reality of these peaks, it may be noted that in the case of stationary noise the distribution of the periodogram is approximately exponential with mean the power spectrum. Using this approximation, one computes that the width of a 95% confidence interval, for the values of Figure 2, is 4.98. The level of fluctuations in Figure 2 is generally greater than this.

2.3 Complex Demodulation

One particularly effective method for assessing the validity of the model (9) and for obtaining initial estimates of the parameters appearing is <u>complex demodulation</u>, see for example Brillinger (1975, Section 2.7.) The basic ideas are: frequency isolation by narrow band filtering to focus on a single term in (9), followed by frequency translation to slow the oscillations down. The steps are: i) $Y(t) \longrightarrow Y(t)\exp\{i\lambda t\}$, (modulation), then ii) smooth $Y(t)\exp\{i\lambda t\}$ to obtain $Y(t,\lambda)$, the complex demodulate at frequency λ. In the case that $Y(t) = \rho\exp\{-\sigma t\}\cos(\gamma t + \delta)$ one has

$$
\begin{aligned}
Y(t,\lambda) &\doteq \tfrac{1}{2}\rho\, e^{i\delta}\, e^{-\sigma t}\, e^{i(\lambda-\gamma)t} && \lambda \text{ near } \gamma \\
&\doteq 0 && \text{otherwise}
\end{aligned}
\tag{12}
$$

Hence $\log |Y(t,\lambda)| \doteq \log \frac{\rho}{2} - \sigma t$ and $\arg\{Y(t,\lambda)\} \doteq \delta + (\lambda-\gamma)t$. Plots of these quantities versus t provide checks on model adequacy and yield estimates of the parameters appearing. In the case that λ is near γ the phase plot will be approximately horizontal. Figures 3 and 4 provide plots at the frequency .0945 cycles/min. (corresponding to one of the peaks in Figure 2.) The results are consistent with an exponentially decaying cosine component. Various other plots for this data set are presented in Bolt and Brillinger (1979).

2.4 Estimation Via Nonlinear Regression

Estimates of parameters are insufficient without accompanying estimates of uncertainty. Fourier inference may be employed to address this problem. Suppose one has a model

$$Y(t) = S(t;\theta) + \varepsilon(t) \tag{13}$$

with $S(\cdot;\theta)$ known up to the finite dimensional parameter θ and with $\varepsilon(\cdot)$ a stationary noise series. Let

$$Y_j = \sum_{t=0}^{T-1} Y(t) \exp\{-i2\pi jt/T\} \tag{14}$$

with similar definitions for $S_j(\theta)$ and ε_j . There are various central limit theorems, (see for example Brillinger (1983)), suggesting that the distribution of ε_j may be approximated by a complex normal with mean 0 and variance $2\pi T f_{\varepsilon\varepsilon}(2\pi j/T)$ and that ε_j, $\varepsilon_{j'}$, $j \neq j'$ are approximately independent. Here $f_{\varepsilon\varepsilon}(\lambda)$ is the <u>power spectrum</u> at frequency λ of the stationary series $\varepsilon(\cdot)$,

$$f_{\varepsilon\varepsilon}(\lambda) = (2\pi)^{-1} \sum_{u=-\infty}^{\infty} \mathrm{cov}\{\varepsilon(t+u),\varepsilon(t)\} \exp\{-i\lambda u\} \tag{15}$$

Supposing $f_{\varepsilon\varepsilon}(\lambda)$ not to vary too much for λ in a neighborhood I, Θ may be estimatined by setting down a Gaussian likelihood and maximizing it. This comes down to minimizing

$$\Sigma \quad |Y_j - S_j(\Theta)|^2 \tag{16}$$

where the summation is over frequencies $2\pi j/T$ in I . For the case of $S(t;\Theta) = \rho \exp\{-\sigma t\}\cos(\gamma t + \delta)$, $\Theta = (\rho,\sigma,\gamma,\delta)$ one finds for example that the asymptotic variance of the estimate of γ is proportional to $T^{-3}\rho^{-2}4\pi\, f_{\varepsilon\varepsilon}(\gamma)$. The details may be found in Bolt and Brillinger (1979) and Hasan (1982). For example, for the Chilean data and the frequency of Figures 3 and 4 one finds, converting frequency to period, an estimated period of 10.5681 min. with an estimated standard error of .0014 min. . Again, details may be found in Bolt and Brillinger (1979).

2.5 Estimation of Bifrequency

Suppose that the system of equations (6) is perturbed by replacing the matrix $\underset{\sim}{A}$ by $\underset{\sim}{A} + \varepsilon\langle \underset{\sim}{B},\underset{\sim}{Y}(t)\rangle$, with ε small and $\langle \underset{\sim}{B},\underset{\sim}{Y} \rangle$ representing a matrix of the same dimensions as $\underset{\sim}{A}$, linear in $\underset{\sim}{Y}$. The solution of the perturbed, now <u>nonlinear</u>, system contains terms in $\exp\{\mu_j t\}$ as at (7), but it also contains interation terms $\exp\{(\mu_k+\mu_\ell)t\}$. A simple form of solution suggested is

$$Y(t) = \sum_{m=1}^{3} \rho_m \cos(\gamma_m t + \delta_m) + \varepsilon(t) \tag{17}$$

where the γ_m are related by $\gamma_1 + \gamma_2 + \gamma_3 = 0$. A triple of frequencies $(\gamma_1, \gamma_2, \gamma_3)$ summing to 0 is referred to as a <u>bifrequency</u>, see Brillinger (1980). The <u>biperiodogram</u> is a statistic of use in detecting the presence of bifrequencies. It is a direct extension of the (second-order) periodogram (11) and is given by

$$I_{YYY}^T(\lambda_1, \lambda_2) = (2\pi)^{-2} T^{-1} d_Y^T(\lambda_1) d_Y^T(\lambda_2) \overline{d_Y^T(\lambda_1 + \lambda_2)} \tag{18}$$

Its modulus may be expected to be large when the frequencies λ_1, λ_2, $\lambda_1 + \lambda_2$ are simultaneously present in the series $Y(\cdot)$.

Zadro and Caputo (1968) develop differential equations for the motion of the Earth in a great earthquake when nonlinearities are present. This work suggests that bifrequencies will be present in that case. Zadro and Caputo (1968) present the results of bispectral computations for the case of the great Alaskan earthquake of 1964. Various suggestive peaks are present in the biperiodogram.

Figure 5 is a contour plot of the modulus of the quantity (18) for the Chilean data and the frequency interval (.08, .12) cycles/min. Peaks are seen to occur both on and off the diagonal $\lambda_1 = \lambda_2$. The largest peak occurs at (.09714, .10459) cycles/min. . If one scans Table 1 in Bolt and Currie (1975) one sees that one may have evidence for the interaction of the torsional vibration modes ${}_0T_{10}$, ${}_0T_{11}$ and ${}_0T_{25}$. The results of Brillinger (1980) and further computations may be employed to assess the uncertainties of these values.

3. NOISE SUSTAINED OSCILLATIONS

3.1 Conceptual Background

Consider the case of incoherent light. A model for this situation is the following: electrons of pertinent atoms jump levels. Light of frequency $\gamma = E/h$ is released where E is the change in energy and h is Plank's constant. The time course of the light signal is $a(t) = H(t)\ e^{-\sigma t}\cos \gamma t$, where $H(t) = 0$ for $t < 0$ and $H(t) = 1$ for $t > 0$. When many atoms are involved the light wave has the form $\sum_j a(t - \tau_j)$, the τ_j being the points of a Poisson process. One is led to consider a process that is a random sum of decaying cosine waves, all waves having the same frequency γ. The power spectrum of this process has poles at $\lambda = \pm\gamma \pm i\sigma$. It will show peaks for λ near γ.

An analagous result obtains for the system (6) when the input process $\underset{\sim}{X}(\cdot)$ is white noise. Suppose $\underset{\sim}{X}(\cdot)$ is white noise with covariance matrix $\underset{\sim}{\Sigma}$. Then the spectral density matrix of the process $\underset{\sim}{Y}(\cdot)$ is given by

$$\frac{1}{2\pi}(\underset{\sim}{A} - i\lambda\underset{\sim}{I})^{-1}\underset{\sim}{\Sigma}(\underset{\sim}{A} + i\lambda\underset{\sim}{I})^{-1} \tag{19}$$

Poles occur for $\lambda = \pm i\mu_j$, the μ_j being the latent values of $\underset{\sim}{A}$. The solution of (6) may be written

$$\begin{aligned} \underset{\sim}{Y}(t) &= \int_0^\infty \exp\{\underset{\sim}{A}u\}\ \underset{\sim}{X}(t-u)\ du \\ &= \sum_j \underset{\sim}{v}_j^\tau \int_0^\infty \exp\{\mu_j u\}\ \underset{\sim}{X}(t-u)\ du\ \underset{\sim}{u}_j \end{aligned} \tag{20}$$

(where $\underset{\sim}{u}_j$, $\underset{\sim}{v}_j$ are the left and right latent vectors of $\underset{\sim}{A}$) and one sees that the process $\underset{\sim}{Y}(\cdot)$ is a random sum of decaying cosine waves frequencies corresponding to the imaginary parts of the latent values of $\underset{\sim}{A}$. Our concern now turns to the estimation of those frequencies. We will proceed via a particular example.

3.2 The Chandler Wobble

The point of intersection of the Earth's axis of rotation with the north polar cap does not remain fixed, rather it wanders about and the Earth is said to "wobble". Figures 6 and 7 give the two coordinates $(X(t),Y(t))$ of the pole for the period 1900 - 1975 . It is convenient to set $Z(t) = X(t) + iY(t)$, then the equations of motion (see Munk and MacDonald (1960)) are

$$\frac{dZ(t)}{dt} = a\, Z(t) + \frac{d\Phi(t)}{dt} \tag{21}$$

with $\Phi(t)$ corresponding to the excitation process. Supposing the process $\Phi(\cdot)$ to have stationary increments, the power spectrum of the process $Z(\cdot)$ is given by

$$\frac{1}{(\lambda-\gamma)^2 + \sigma^2} f_{\Phi\Phi}(\lambda) \tag{22}$$

writing $a = i\gamma - \sigma$. The periodogram of the data of Figures 6,7 is given in Figure 8 . It shows peaks near frequencies 0, .071 and .083 cycles/year. The first correspond to trend - see Figure 7. The third corresponds to an annual component - present in the excitation process. The second corresponds to the Chandler wobble - to γ of (22) . It is of interest to estimate the Chandler period precisely and to provide a measure of uncertainty.

A corresponding finite parameter model is developed in Brillinger (1973). Specifically for seasonally adjusted first differences and measurment error assumed present, the following parametric spectrum is derived

$$\frac{\sigma^2}{2\pi}\ \frac{1-e^{-2\sigma}}{2\sigma}\ \frac{1}{1-2\exp\{-\sigma\}\cos(\lambda-\gamma)+\exp\{-2\sigma\}} + \frac{\psi^2|1-e^{-i\lambda}|^2}{2\pi} \qquad (23)$$

This is then fit (to the data for 1902-1969) by the method of Gaussian estimation, that is by maximizing the "Gaussian" likelihood

$$\prod_j \frac{1}{f_j} \exp\{-I_j^T/f_j\} \qquad (24)$$

where I_j^T denotes the periodogram at frequency $2\pi j/T$ and $f_j = f(\frac{2\pi j}{T};\theta)$ denotes the theoretical power spectrum as a function of the unknown parameters. This method also leads to estimated standard errors. In particular the value $\hat{\gamma} = .0706$ with an estimated standard error of .0026 was found.

Further examination of the periodogram of Figure 8 shows some power near the frequency .15 . It was examined further with a suspicion that it might be due to some nonlinearity. Figures 9, 10 provide the results of complex demodulating the series at a frequency of .153 cycles/year. It was found that the power was predominantly present only for the early part of the series. We have no explanation to present beyond remarking that the individuals responsible for estimating the polar motion changed every so often. The biperiodogram is presented in Brillinger (1973), but it is not strongly suggestive of a nonlinearity.

3.3 Nuclear Magnetic Resonance

3.3.1 The Bloch Equations. Nuclear magnetic resonance relies on the interaction between magnetically sensitive nuclei which are exposed to both a strong magnetic field and a radio frequency signal. The nuclei "flip" at characteristic (or resonant) frequencies. The procedure yields information related to molecular structure, interactions and dynamics.

The phenomenon has been described by the Bloch equations. These take the form

$$\frac{d\underset{\sim}{Y}(t)}{dt} = \underset{\sim}{a} + \underset{\sim}{A}\,\underset{\sim}{Y}(t) + \underset{\sim}{B}\,\underset{\sim}{Y}(t)\,X(t) \tag{25}$$

with $X(t)$ scalar input, with $\underset{\sim}{Y}(t)$ vector output, with $\underset{\sim}{a}$ a vector and with $\underset{\sim}{A}$, $\underset{\sim}{B}$ matrices. See, for example, Knight and Kaiser (1982).

Various inputs have been employed to identify molecular systems by nuclear magnetic resonance. These include pulses, cosinusoids and noise. The impulse response has been written

$$\sum_k \underset{\sim}{\rho}_k \exp\{-\sigma_k t\} \cos \gamma_k t \tag{26}$$

with the γ_k the characteristic frequencies of the substance of concern. One common procedure is to apply a pulse and to the look for peaks in the absolute value (periodogram) of the Fourier transform of the output. Peaks are assigned to particular atoms in the molecules present.

3.3.2 Stochastic Nuclear Magnetic Resonance. In stochastic NMR the input, $X(\cdot)$, is taken to be random noise and the particular realization is made use of in the analysis. Blumich (1985) provides a review. In the case that the input is Gaussian white noise, $\mathrm{cov}\{\underset{\sim}{Y}(t+u), X(t)\}$ is found to be given by

$$\sum_k \underset{\sim}{\rho}_k \exp\{-\sigma_k u\} \exp\{i\gamma_k u\} \tag{27}$$

for $u > 0$ with the $i\gamma_k - \sigma_k$ the latent values of $\underset{\sim}{A} + \underset{\sim}{B}^2/2$. The Fourier transform of (27) is

$$\sum_k \underset{\sim}{\rho}_k \frac{1}{\sigma_k - i(\lambda - \gamma_k)} \tag{28}$$

The amplitude of this quantity peaks at λ near γ_k and sample-based quantities may be used to derive estimates. Examples may be found in Ernst (1970).

In many important cases second-order spectra are not sufficient to describe structure unequivocally, higher-order spectra are needed. Because of symmetries present, third-order spectra vanish identically. The fourth-order spectrum, which is the Fourier transform of $E\{\underset{\sim}{Y}(t)X(t+u_1)X(t+u_2)X(t+u_3)\}$, has peaks when the frequencies γ_j, γ_k, γ_ℓ and $\gamma_j+\gamma_k+\gamma_\ell$ are simultaneously present. Examples of sections of such empirical spectra are given in Blumich and Ziessow (1983). The use of such spectra is found to lead to near complete assignment of protons to molecules in many substances of concern.

3.4 Particle Processes

Consider a circumstance in which at time t there are $N(t)$ particles situated in space at the locations $\underset{\sim}{r}_j(t)$, $j = 1,\cdots,N(t)$. If $\underset{\sim}{r}$ denotes position in space, then this particle process may be represented by

$$\sum_{j=1}^{N(t)} \delta(\underset{\sim}{r} - \underset{\sim}{r}_j(t)) \tag{29}$$

The motion of the j-th particle may be described via $\underset{\sim}{r}_j(t)$. For example if the particle is moving with a constant (directed) velocity then $\underset{\sim}{r}_j(t) - \underset{\sim}{r}_j(0) = \underset{\sim}{v}\, t$. If the particles motion is Brownian, then $\underset{\sim}{r}_j(t)$ is a spatial Brownian motion with independent Gaussian increments.

With the advent of lasers, the motion of collections of particles may be studied by analysing light scattered when the particles are illuminated by a laser. Briefly through the Doppler effect the frequency of the incident light is shifted slightly by a particles motion and a study of the frequency distribution of the scattered light gives information on the velocity distribution of the particles.

3.4.1 Laser Doppler Velocimetry. The characteristic property of monochromatic laser light is that it fluctuates very nearly as a cosine wave. Suppose that the incident light comes from a direction $\underset{\sim}{k}_I$ and has frequency ω. Then the input to the particle system may be represented as

$$X(t) = \exp\{ i(\underset{\sim}{k}_I \cdot \underset{\sim}{r} + \omega t) \tag{30}$$

Further the (far-field) scattered output in a direction $\underset{\sim}{k}_S$ may be represented as $Y(t) = s_{\underset{\sim}{K}}(t)\, X(t)$ where $\underset{\sim}{K} = \underset{\sim}{k}_S - \underset{\sim}{k}_I$ and $s_{\underset{\sim}{K}}(t)$ the complex scattering amplitude is given by

$$s_{\underset{\sim}{K}}(t) = \sum_j a_j(t) \exp\{-i \underset{\sim}{K} \cdot \underset{\sim}{r}_j(t)\} \tag{31}$$

Here $X(t)$, $Y(t)$ represent the incident and scattered optical fields and $a_j(t)$ is referred to as the form factor. Supposing that the particles are independent and identical and that the $a_j(\cdot)$ are independent of the $\underset{\sim}{r}_j(\cdot)$ one sees that the autocovariance function of the process $Y(\cdot)$ is given by

$$\begin{aligned} m_{YY}(u) &= E\{s_{\underset{\sim}{K}}(t+u)\ \overline{s_{\underset{\sim}{K}}(t)}\} \\ &\sim E\{\exp\{-i\underset{\sim}{K}\cdot(\underset{\sim}{r}(t+u) - \underset{\sim}{r}(t))\}\} \end{aligned} \tag{32}$$

It is essentially the characteristic function of the increments of the motion of the particle process. Supposing one has constant (laminar) flow, then $m_{YY}(u) \sim \exp\{-i\ \underset{\sim}{K}\cdot\underset{\sim}{v}u\}$. Supposing Brownian motion, $m_{YY}(u) \sim \exp\{-DK^2u\}$ with D the diffusion constant and $K = |\underset{\sim}{K}|$. Other models for the motion of the particles, eg. mixtures of particles with different velocities or different diffusion constants, lead to other functional forms for $m_{YY}(\cdot)$. The problem now is, how to estimate $m_{YY}(u)$ in practice.

The nature of the situation is that the electric field, $Y(\cdot)$, cannot be observed directly. What can be observed are Poisson processes with rate the modulus-squared of an electric field. In one experimental setup a Poisson process with rate $I(t) = |Y(t)|^2 = |s_{\underset{\sim}{K}}(t)|^2$ is observed. The number of particles, N, is assumed large so that $s_{\underset{\sim}{K}}(t)$ of (31) is approximately Gaussian. From Isserlis's formula then

$$m_{II}(u) = |m_{YY}(0)|^2 + |m_{YY}(u)|^2 \tag{33}$$

and from an estimate of $m_{II}(u)$, an estimate of $|m_{YY}(u)|^2$ may be constructed. This procedure may be employed successfully for particles moving with Brownian motion, see for example Nishio et al. (1983); however in the case of laminar flow $m_{YY}(u) \sim \exp\{-i\,\underset{\sim}{K}\cdot\underset{\sim}{v}u\}$, whose modulus contains no information on $\underset{\sim}{K}$. The experimental setup has to be altered.

In Doppler-difference velocimetry: the frequency ω of the input beam is shifted slightly to $\omega+\delta$ giving a second input $X'(t)$ coming from a different direction and the far-field intensity is then

$$I(t) = |s_{\underset{\sim}{K}}(t)X(t) + s_{\underset{\sim}{K}'}(t)X'(t)|^2 \tag{34}$$

Expanding this shows

$$I(t) \sim \exp\{i(\underset{\sim}{K} - \underset{\sim}{K}')\cdot\underset{\sim}{v}t\} \exp\{-i\delta t\} + \cdots \tag{35}$$

in the case of laminar flow and the problem has again become one of estimating the frequency of a cosine. This procedure is made use of in Pfister et al. (1983) and Sato et al. (1978) for example. An important advantage of this experimental technique is that rapidly varying velocities may be tracked and even subjected to Fourier analyses themselves (see Pfister et al. (1983).)

Cummins (1977) and Schulz-DuBois (1983) are general references to the techniques and uses of laser velocimetry.

3.4.2 Discussion. It is worth remarking that the interference procedure made use of is intimately connected to the technique of complex demodulation described earlier in the paper. By superposing the $X'(t)$ signal one is essentially bringing about multiplication by $\exp\{i(\omega+\delta)t\}$ allowing, as in the case of complex demodulation, attention to be focused on components of frequency near ω.

In the case that the intensity $I(t)$ is low, sampling fluctuations will need to be taken account of.

3.4.3 Bispectral Analysis. In an interesting piece of work Sato et al. (1978) combine laser Doppler velocimetry with bispectral analysis to obtain information concernin particles in suspension. Their approach has the advantage of "eliminating" Gaussian noise.

The experimental set-up involved: vibrating particles (in one case cigar smoke, inanother water) by a known sound wave

$$X(t) = A_1 \sin(\omega_0 t + \Phi_1) + A_2 \sin(2\omega_0 t + \Phi_2) \tag{36}$$

and then measuring the particle motion by a laser Doppler velocimeter. The measured signal takes the form

$$Y(t) = a_1 \sin(\omega_0 t + \phi_1) + a_2 \sin(2\omega_0 t + \phi_2) + \varepsilon(t) \tag{37}$$

with the a_i functions of A_1, A_2, particle diameter, relative density of particle material, viscosity of the medium and other things. The series $\varepsilon(\cdot)$ represents noise.

The power spectrum of $Y(\cdot)$ is given by

$$\frac{1}{4\pi}\left(a_1^2\, \delta(\lambda - \omega_0) + a_2^2\, \delta(\lambda - 2\omega_0)\right) + f_{\varepsilon\varepsilon}(\lambda) \tag{38}$$

and it should be noted that the noise spectrum appears. Supposing the noise to be Gaussian, in contrast the amplitude of the bispectrum is

$$\frac{1}{32\pi^2}\, a_1^2\, |a_2|\, \delta(\lambda_1 - \omega_0)\, \delta(\lambda_2 - \omega_0) \tag{39}$$

and the noise component is absent. The value $a_1^2|a_2|$ may be estimated from the bispectral estimate and used in turn to estimate particle parameters. Sato et al. (1978) present experimental results demonstrating that this bispectrum based estimate can be much more sensitive than a power spectrum based one.

4. DISPERSION AND MODES

4.1 Background

Consider the linear-temporal process

$$Y(x,t) = \rho \cos(\alpha x + \gamma t + \delta) \tag{40}$$

It satisfies the wave equation

$$\frac{\partial^2 Y}{\partial t^2} = c^2 \frac{\partial^2 Y}{\partial x^2} \tag{41}$$

with $c = \gamma/\alpha$, the phase velocity. In the case that there are side conditions, following Sturm-Liouville theory, discreteness occurs. Given frequency γ only a certain number of wavenumbers $\alpha = \alpha_n(\gamma)$, $n = 0, 1, \ldots$ are possible. An implication of this is that for a composite wave different frequency components will travel at different speeds, or disperse. Such a relation between frequency and wavenumber is referred to as a dispersion relation.

From a statistical viewpoint the following problem arises, given data on $Y(x,t)$ and imagining it to be a superposition of terms of the form (40) satisfying a dispersion relation, how is that relation to be estimated? It is instructive to consider the (two-dimensional) Fourier transform.

One has

$$\iint \exp\{i(\alpha(\gamma)x+\gamma t)\} \exp\{-i(kx+\lambda t)\} \, dx \, dt = \delta(\lambda-\gamma)\, \delta(k-\alpha(\gamma)) \tag{42}$$

Mass is seen to occur on the curve $k = \alpha(\lambda)$. In the case of a composite process, mass may be expected to occur on a family of curves $k = \alpha_n(\lambda)$.

4.2 Examples

The fields of oceanography, seismology and helioseismology provide empirical examples of the use of Fourier transforms to discern dispersion relations. Gilbert and Dziewonski (1975) provide analyses for the free oscillations of the earth based on seismograms from two deep earthquakes. Munk et al. (1964) analysed sea level fluctuations as measured by a linear array of gauges off the coast of Southern California. Estimating a wavenumber-frequency power spectrum, they found most of the energy to be trapped in a few narrow bands in (k,λ) space, corresponding to edge waves. (These are water waves moving sideways to the shore, rather than rolling on to it.)

The most dramatic developments have however been taking place in the field of helioseismology, that is the branch of solar physics concerned with the study of resonant oscillations of the Sun. The motion of the visible portion of the Sun's surface is measured via spectrographs attached to conventional solar telescopes. Velocity of movement is determined through the Doppler effect. The wavenumber-frequency power spectrum is then estimated from the data. The cover of the 6 September issue of Science provides a striking example of such an estimate. References to this work include Deubner and Gough (1984), Christensen-Dalsgaard et al. (1985) .

4.3 Discussion

Given a model (eg. velocity as a function of depth) for the medium of interest, implied dispersion curves may be computed (see for example Section 7.2.2 in Aki and Richards (1980)). The empirically determined wavenumber-frequency power spectrum may then be employed to assess the degree of fit of the postulated model. Further one may set up an inverse problem and proceed to improve the model.

The excitement with which researchers view helioseismology is well illustrated by the following remarks in Deubner et al. (1975) :
"... the basic mechanism responsible for the solar 5-minute oscillation is now understood,..." and "... the solutions in Ulrich agree with the observed ridges in all detail to an embarassin extent."

5. A REVIEW OF SOME PARTICULAR RESULTS

In this section the crude details of a variety of results, concerning the fitting of cosine type signals superposed on stationary mixing noise, are presented.

5.1 Whittle (1952)

The model considered is

$$Y(t) = \alpha \cos(\gamma t + \delta) + \varepsilon(t) \tag{43}$$

$t = 0, \ldots, T-1$. The difficult parameter to estimate is γ. It may be estimated either by ordinary least squares or more commonly by maximizing the periodogram

$$\left| \sum_{t=0}^{T-1} Y(t)\, e^{-i\lambda t} \right|^2 \tag{44}$$

The estimate $\hat{\gamma}$ is found to be asymptotically normal with mean γ and variance

$$\frac{48\pi}{T^3 \alpha^2} f_{\varepsilon\varepsilon}(\gamma) \tag{45}$$

That the variance falls off as T^{-3} was initially suprising. Hannan (1971,3) and Walker (1971,3) are related papers.

5.2 Bolt and Brillinger (1979)

This work was referred to earlier in the paper. The model considered is

$$Y(t) = \alpha\, e^{-\phi t/T} \cos(\gamma t + \delta) + \varepsilon(t) \tag{46}$$

$t = 0,\cdots,T-1$. The parameters are estimated from the (Gaussian) likelihood of the Fourier transform values in the neighborhood of γ . The estimates $\hat{\gamma}$ and $\hat{\phi}/T$ are found to be asymptotically normal with variance

$$\frac{4\pi}{T^3\alpha^2} f_{\varepsilon\varepsilon}(\gamma) \int_0^1 e^{-2\phi u}du \Big/ \left[\int_0^1 e^{-2\phi u}du \int_0^1 u^2 e^{-2\phi u}du - \left\{ \int_0^1 u e^{-2\phi u}du \right\}^2 \right] \tag{47}$$

The parametrization of the decay rate in the form ϕ/T is in order to insure that the signal does nor drop out asymptotically. It seems a plausible manner in which to develop asymptotic results.

5.3 Hinich and Shaman (1972)

The work of these researchers is concerned with an areal-temporal process. The model is

$$Y(x,y,t) = \rho \cos(\alpha x + \beta y + \gamma t + \delta) + \varepsilon(x,y,t) \tag{48}$$

for x, y, t taking on values in a latice. Ordinary least squares, maximum likelihood and periodogram maximizing estimates are considered.

5.4 Vere-Jones (1982)

He was concerned with fitting a cyclic model to point process data. A point process $\{\tau_j\}$ is assumed to be Poisson with rate $A \exp\{\alpha \cos(\gamma t + \delta)\}$. The asymptotic distributions of the maximum likelihood estimate and a periodogram maximizing estimate are developed. The asymptotic distribution of $\hat{\gamma}$ is found to be normal with mean γ and variance $12/[T^3 A \alpha I_1(\alpha)]$. Here $I_1(\alpha)$ is a modified Bessel function.

5.5 Isokawa (1983)

This author is concerned with sampled time series data, $Y(\tau_j)$, where the τ_j are the points of a realization of a stationary point process independent of the series $Y(t)$ given by (43) . The asymptotic distribution of the estimate of λ maximizing the periodogram

$$\left| \sum_j Y(\tau_j) \exp\{-i\lambda\tau_j\} \right|^2 \tag{49}$$

is determined.

5.6 Hannan (1974)

In this paper Hannan presents results for the model

$$Y(t) = \sum_k \alpha_k \cos(k\gamma t + \delta_k) + \varepsilon(t) \tag{50}$$

$t = 0,\ldots,T-1$. The import of this model is that the expected value has period $2\pi/\gamma$. The asymptotic distribution of the λ maximizing

$$\sum_k |d_Y^T(k\lambda)|^2/f_{\varepsilon\varepsilon}(k\lambda) \tag{51}$$

is derived. It is found to be normal with mean and variance

$$1/[\, T^3 \sum_k \alpha_k^2/(48\pi\, f_{\varepsilon\varepsilon}(k\gamma))\,] \tag{52}$$

In practice an estimate of $f_{\varepsilon\varepsilon}(\cdot)$ would be inserted in (51) .

5.7 Brillinger (1980)

This work was referred to earlier. The model is

$$Y(t) = \sum_{k=1}^{3} \alpha_k \cos(\gamma_k t + \delta_k) + \varepsilon(t) \tag{53}$$

with $\gamma_3 = \gamma_1 + \gamma_2$ or $= 2\pi - \gamma_1 - \gamma_2$, $0 < \gamma_k < \pi$. This is the model of bifrequencies. The asymptotic distributions of both the ordinary least squares estimate and the estimate (λ_1, λ_2) maximizing the biperiodogram

$$d_Y^T(\lambda_1)\ d_Y^T(\lambda_2)\ \overline{d_Y^T(\lambda_1 + \lambda_2)} \tag{54}$$

are determined. The asymptotic distributions are found to be normal, but to be different generally.

5.8 Subba Rao and Yar (1982)

These researchers are concerned with the model of frequency modulation,

$$Y(t) = \alpha \cos(\gamma t + \delta + \zeta \sin(\psi t + \nu)) + \varepsilon(t) \tag{55}$$

Estimates of γ, ψ are determined by maximizing

$$\sum_k |d_Y^T(\gamma + k\psi)|^2 / f_{\varepsilon\varepsilon}(\gamma + k\psi) \tag{56}$$

5.9 Brillinger (1985)

This work considers the areal-temporal process (48), but now the sensors are irregularly distributed at locations (x_j, y_j), $j = 1, \cdots, J$. The time period T is thought of as large, and so γ may be treated as known. If

$$\underset{\sim}{Y}_k = \frac{1}{T} \sum_{t=0}^{T-1} [\, Y(x_j, y_j, t)]\ \exp\{-i\frac{2\pi k t}{T}\} \tag{57}$$

$$\underset{\sim}{M} = \Sigma\ \underset{\sim}{Y}_k \overline{\underset{\sim}{Y}}_k^{\tau} \tag{58}$$

the summation being over Fourier frequencies $2\pi k/T$ near γ and

$$\underset{\sim}{S} = \underset{\sim}{M} - \underset{\sim}{Y}_{k'}\overline{\underset{\sim}{Y}}_{k'}^{\tau} \tag{59}$$

with $2\pi k'/T = \gamma$. (This last is an estimate of the spectral density matrix of the J noise process $\varepsilon(x_j,y_j,t)$). Finally define the (steering) vector

$$\underset{\sim}{B} = [\exp\{i(\alpha x_j + \beta y_j)\}] \tag{60}$$

(In (57) and (60) the $[\cdot]$ notation denotes a J column vector.) The estimate studied is the (α,β) maximizing the 'likelihood ratio detection' statistic

$$\frac{\overline{\underset{\sim}{B}}^{\tau}\underset{\sim}{S}^{-1}\underset{\sim}{B}}{\overline{\underset{\sim}{B}}^{\tau}\underset{\sim}{M}^{-1}\underset{\sim}{B}} - 1 \tag{61}$$

The asymptoic distribution of the estimate is indicated.

5.10 Brillinger (1986)

The previous situation may be viewed as corresponding to a small array of sensors. The work in this reference concerns a large array case, with the measurements irregularly placed with respect to all coordinates. It is convenient to alter the notation somewhat. Suppose

$$Y(t) = a\cos(\omega,t) + b\sin(\omega,t) + \varepsilon(t) \tag{62}$$

for ω, t in R^p and $(\omega,t) = \omega_1 t_1 + \cdots + \omega_p t_p$. Suppose the data available are the values $\{\tau_j, Y(\tau_j)\}$ for τ_j in a region $\mathcal{J}$. The parameter ω is estimated by maximizing, for λ in R^p

$$|\sum_j \exp\{-i(\lambda,\tau_j)\}\, Y(\tau_j)|^2 \tag{63}$$

and given $\hat{\omega}$, (a,b) estimated by ordinary least squares. Asymptotic distributions are obtained assuming $\{\tau_j\}$ is a realization of a stationary mixing point process in R^p with rate c_N and spectrum $f_{NN}(\lambda)$. In particular the estimates are found to be asymptotically normal with covariance matrix

$$c_N^{-2} 2(2\pi)^p f_{VV}(\lambda) \, \underset{\sim}{\Sigma}_T^{-1} \tag{64}$$

where $f_{VV}(\lambda) = c_N^{-2} f_{\varepsilon\varepsilon}(\lambda) + \int f_{NN}(\lambda-\alpha) f_{\varepsilon\varepsilon}(\alpha) d\alpha$ and

$$\underset{\sim}{\Sigma}_T = \begin{bmatrix} |\mathcal{T}| & 0 & \beta\int t\,dt \\ 0 & |\mathcal{T}| & -\alpha\int t\,dt \\ \beta\int t^\tau dt & -\alpha\int t^\tau dt & |\rho|^2 \int t^\tau t\,dt \end{bmatrix} \tag{65}$$

The integrals appearing are over the region $\mathcal{T}$. The asymptotics are as $|\mathcal{T}| \to \infty$.

6. SOME OPEN PROBLEMS

We end by indicating in cursory form a number of research problems related to the topic of the paper.

1. Diagnostics, influence, robust/resistant procedures.
2. Missing values, quantization, jitter.
3. Estimation of dimension, eg. by AIC.
4. Inverse problem formulations, ridge regression.
5. Local asymptotic normality, contiguity.
6. Adaptive procedures.
7. The absorbtion model.
8. Signal dependent noise.

9. Law of the iterated logarithm, large deviations, rates of convergence for the estimates.

10. Random effects models.

11. Vector-valued cases.

12. Partially parametric formulations, eg. the periodic case.

13. Models for the point process and telegraph signal cases.

14. Expansions for distributions.

15. Distributions of test statistics, eg. of

$$\sup_{\rho,\lambda} |\Sigma\, \rho^t e^{-i\lambda t}\, Y(t)|^2 / \Sigma\, \rho^{2t} \tag{66}$$

or of

$$\sup_{\lambda_1,\lambda_2} \min \{ I^T(\lambda_1),\ I^T(\lambda_2),\ I^T(\lambda_1+\lambda_2) \} \tag{67}$$

16. Properties of the estimates when the model is untrue.

17. The broadband signal case.

18. Parametric analysis of the quefrency case.

19. Distribution in the null case of sup over (α,β) of (61).

20. Sampling properties of the NMR estimates.

ACKNOWLEDGEMENT

This research was supported by the NSF Grant DMS-8316634.

REFERENCES

Aki, K. and P. G. Richards: 1980, Quantitative Seismology, Freeman, San Francisco.

Blumich, B.: 1985, 'Stochastic NMR spectroscopy', Bulletin Magnetic Resonance 7

Blumich, B. and Ziessow, D. : 1983, 'Nonlinear noise analysis in nuclear magnetic resonance spectroscopy. 1D, 2D, and 3D spectra', J. Chemical Physics 78, 1059-1076.

Bolt, B. A.: 1982, Inside the Earth, Freeman, San Francisco.

Bolt, B. A. and D. R. Brillinger: 1979, 'Estimation of uncertainties in eigenspectral estimates from decaying geophysical time series', Geophysical Journal Royal Astronomical Society 58, 593-603.

Bolt, B. A. and R. G. Currie: 1975, 'Maximum entropy estimates of Earth torsional eigenperiods from 1960 Trieste data', Geophysical Journal Royal Astronomical Society 40, 107-114.

Brillinger, D. R.: 1973, "An empirical investigation of the Chandler wobble", Bulletin International Statistical Institute 45, 413-433.

Brillinger, D. R.: 1975, Time Series: Data Analysis and Theory, Holt, Rinehart and Winston, New York.

Brillinger, D. R.: 1980, 'The comparison of least squares and third-order periodogram procedures in the estimation of bifrequency', Journal of Time Series Analysis 1, 95-102.

Brillinger, D. R.: 1983, 'The finite Fourier transform of a stationary process', in D. R. Brillinger and P. R. Krishnaiah (eds.) Handbook of Statistics 3, Elsevier, Amsterdam, pp. 21-37.

Brillinger, D. R.: 1985, 'A maximum likelihood approach to frequency-wavenumber analysis', IEEE Trans. Acoust. Speech Signal Proc. ASSP-33,

Brillinger, D. R.: 1986, 'Regression for randomly sampled spatial series: the trigonometric case', Essays in Time Series and Allied Processes (eds. J. Gani and M. B. Pristley), Applied Probability Trust.

Clairaut, A.-C.: 1754, 'Mémoire sur l'orbite apparente du soleil autour de la terre, en ayant égard aux perturbations produites par les actions de la lune et des planètes principales', Mémoires de Mathematique et de Physique de l'Académie Royale des Sciences, no. 9, 521-564.

Christensen-Dalsgaard, J., D. Gough and J. Toomre: 1985, 'Seismology of the Sun', Science 229, 923-931.

Cummins, H. Z.: 1977, 'Intensity fluctuation spectroscopy of motile micro-organisms', in H. Z. Cummins and E. R. Pike (eds.) Photon Correlation Spectroscopy and Velocimetry, Plenum, New York.

Deubner, F-L, and D. Gough: 1984, 'Helioseismology', Ann. Rev. Astron. Astrophys. 22, 593-619.

Deubner, F-L., R. K. Ulrich and E. J. Rhodes: 1979, 'Solar p-mode oscillations as a tracer of radial differential rotation', Astron. Astrophys. 72, 177-185.

Ernst, R. R.: 1970, 'Magnetic resonance with stochastic excitation', J. Magnetic Resonance 3, 10-27.

Gilbert, F. and A. M. Dziewonski: 1975, 'An application of normal mode theory to retrieval of structural parameters and source mechanisms from seismic spectra', Philos. Trans. Royal Soc. London A278, 187-269.

Hannan, E. J.: 1971, 'Non-linear time series regression', J. Appl. Prob. 8, 767-780.

Hannan, E. J.: 1973, 'The estimation of frequency', J. Appl. Prob. 10, 510-519.

Hannan, E. J.: 1974, 'Time series analysis', IEEE Trans. Aut. Control AC-19, 706-715.

Hasan, T.: 'Nonlinear time series regression for a class of amplitude modulated cosinusoids', Journal of Time Series Analysis 3, 109-122.

Hinich, M. J. and P. Shaman: 1972, 'Parameter estimation for an R-dimensional plane wave observed with additive independent Gaussian errors', Ann. Math. Statist. 43, 153-169.

Heideman, M. T., D. H. Johnson and C. S. Burrus: 1984, 'Gauss and the history of the fast Fourier transform', IEEE ASSP Magazine, 14-21.

Isokawa, Y.: 1983, 'Estimation of frequency by random sampling', Ann. Inst. Statist. Math. 35, 201-213.

Knight, W. R. and R. Kaiser: 1982, 'The randomly driven Bloch equations', J. Magnetic Resonance 48, 293-301.

Munk, W. H. and G. J. F. MacDonald: 1960, The Rotation of the Earth, Cambridge University Press, Cambridge.

Munk, W., F. Snodgrass and F. Gilbert: 1964, 'Long waves on the continental shelf: an experiment to separate trapped and leaky modes', J. Fluid Mechanics 20, 529-554.

Nishio, I., T. Tanaka, S-T Sun, Y. Imanishi and S. T. Ohnishi: 1983, 'Hemoglobin aggregation in single red blood cells of sickle cell anemia', Science 220, 1173-1175.

Pfister, G., U. Gerdts, A. Lorenzen and K. Schatzel: 1983, 'Hardware and software implementation of on-line velocity correlation measurements in oscillatory and turbulent rotational couette flow' in E. O. Schulz-DuBois, Photon Correlation Techniques, Springer-Verlag, Berlin, pp. 256-262.

Sato, T., T. Kishimoto and K. Sasaki: 1978, 'Laser Doppler particle measuring system using nonsinusoidal forced vibration and bispectral analysis', Applied Optics 17, 667-670.

Schulz-DuBois, E. O. (ed.): 1983. Photon Correlation Techniques, Springer-Verlag, Berlin.

Subba Rao, T. and M. Yar; 1982, 'Statistical analysis of frequency modulated signals', Tech. Report No. 153, Mathematics Dept., University of Manchester Institute of Science and Technology.

Vere-Jones, D.: 1982, 'On the estimation of frequency in point process data', Essays in Statistical Science (eds. J. Gani and E. J.Hannan), Applied Probability Trust.

Walker, A. M.; 1971, 'On the estimation of a harmonic component in a time series with stationary independent residuals', Biometrika 58, 21-36.

Walker, A. M.: 1973, 'On the estimation of a harmonic component in a time series with stationary dependent residuals', Adv. Appl. Prob. 5, 217-241.

Whittle, P.: 1952, 'The simultaneous estimation of a time series' harmonic components and covariance structure', Trab. Estadist. 3, 43-57.

Zadro, M. B. and M. Caputo: 1968, 'Spectral, bispectral analysis and Q of the free oscillations of the Earth', Nuovo Cimento Suppl. 6, 67-81.

Legends

Figure 1. Record of the Chilean earthquake of 22 May 1960 recorded at Trieste. The tides have been removed from the original seismogram.

Figure 2. The natural logarithm of the periodogram of the data of Figure 1. Only part is shown.

Figure 3. The result of complex demodulating the record of Figure 1. The logarithm of the running amplitude is shown. Time is time since onset of the earthquake.

Figure 4. As for Figure 3 except that the running phase is plotted.

Figure 5. The modulus of the biperiodogram of the data of Figure 1. Only part is shown.

Figure 6. The x-coordinate of the position of the Earth's axis of rotation (Northern Hemisphere).

Figure 7. The y-coordinate of the position of the Earth's axis of rotation (Northern Hemisphere).

Figure 8. The natural logarithm of the periodogram of the data of Figures 6 and 7. Only part is shown.

Figure 9. The result of complex demodulating the data of Figures 6 and 7. The logarithm of the running amplitude is shown.

Figure 10. As in Figure 9 except the running phase is shown.

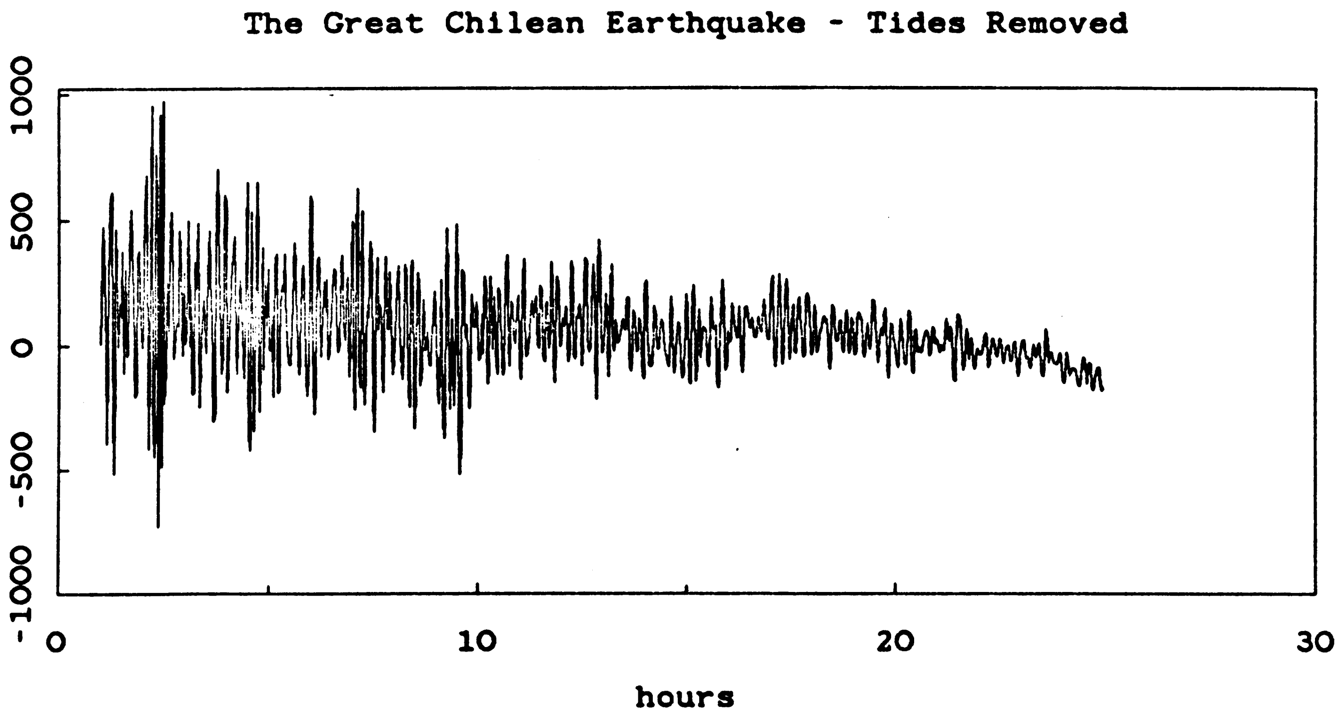

The Great Chilean Earthquake - Tides Removed
1000
500
0
-500
-1000
0
10
20
30
hours

Fig. 1

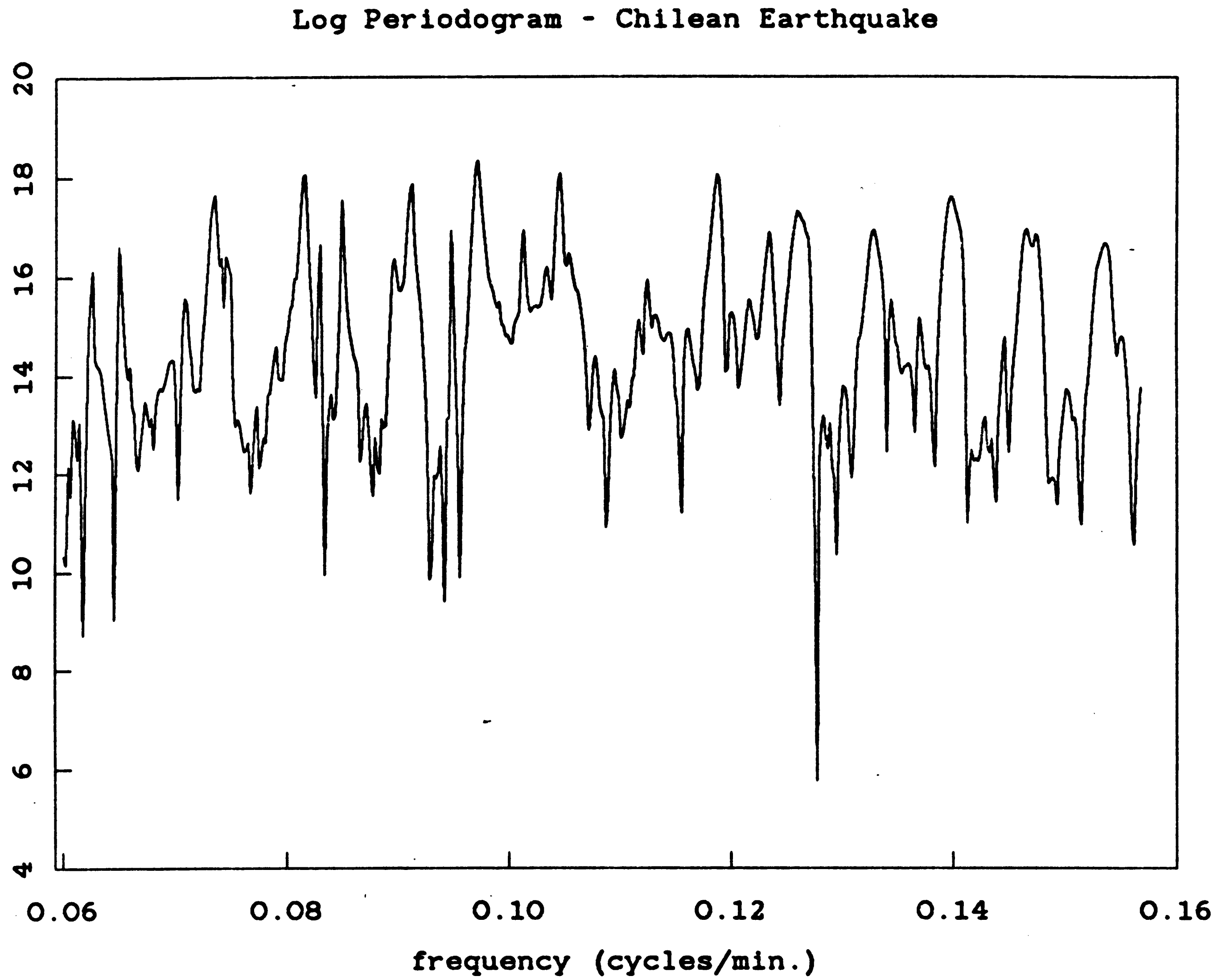
Log Periodogram - Chilean Earthquake
20
18
16
14
12
10
8
6
4
0.06
0.08
0.10
0.12
0.14
0.16
frequency (cycles/min.)

Fig. 2

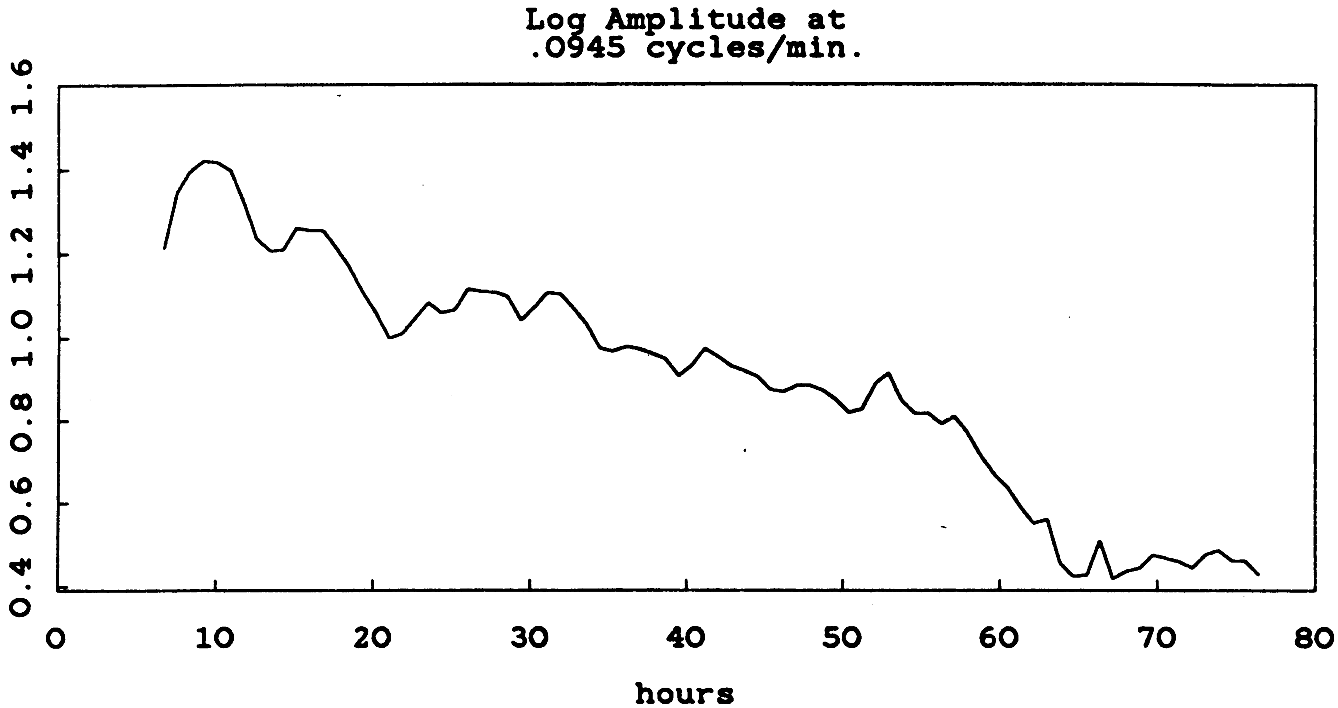
Log Amplitude at
.0945 cycles/min.
0.4 0.6 0.8 1.0 1.2 1.4 1.6
0
10
20
30
40
50
60
70
80
hours

Fig. 3

Phase at .0945 cycles/min.

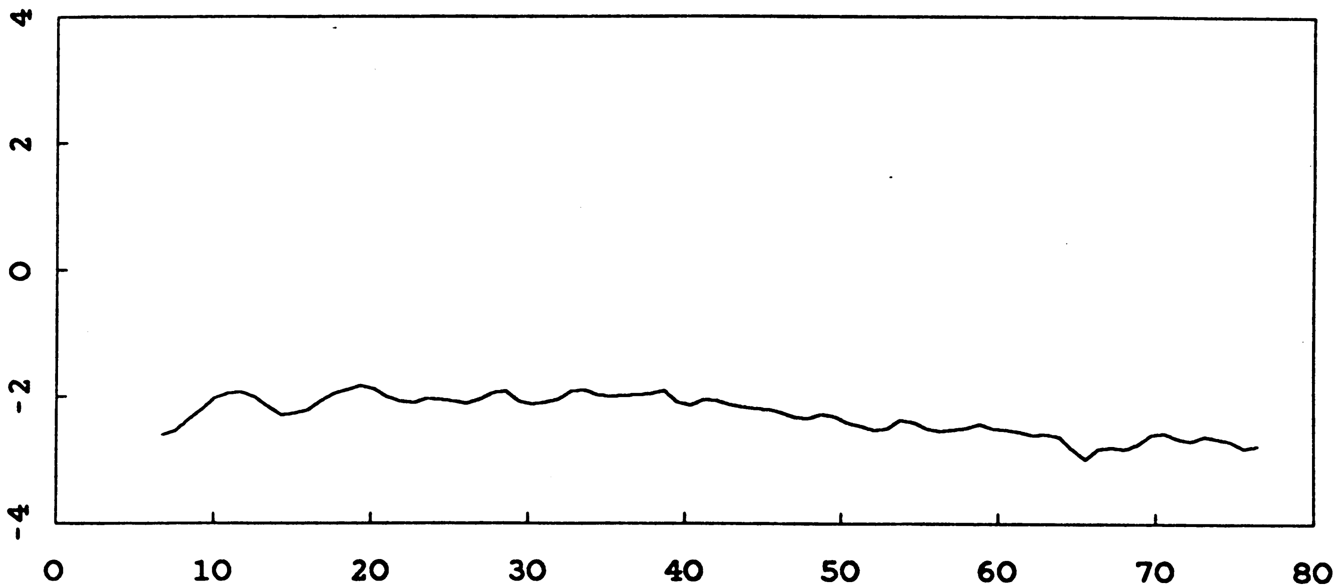

Fig. 4

Modulus Biperiodogram

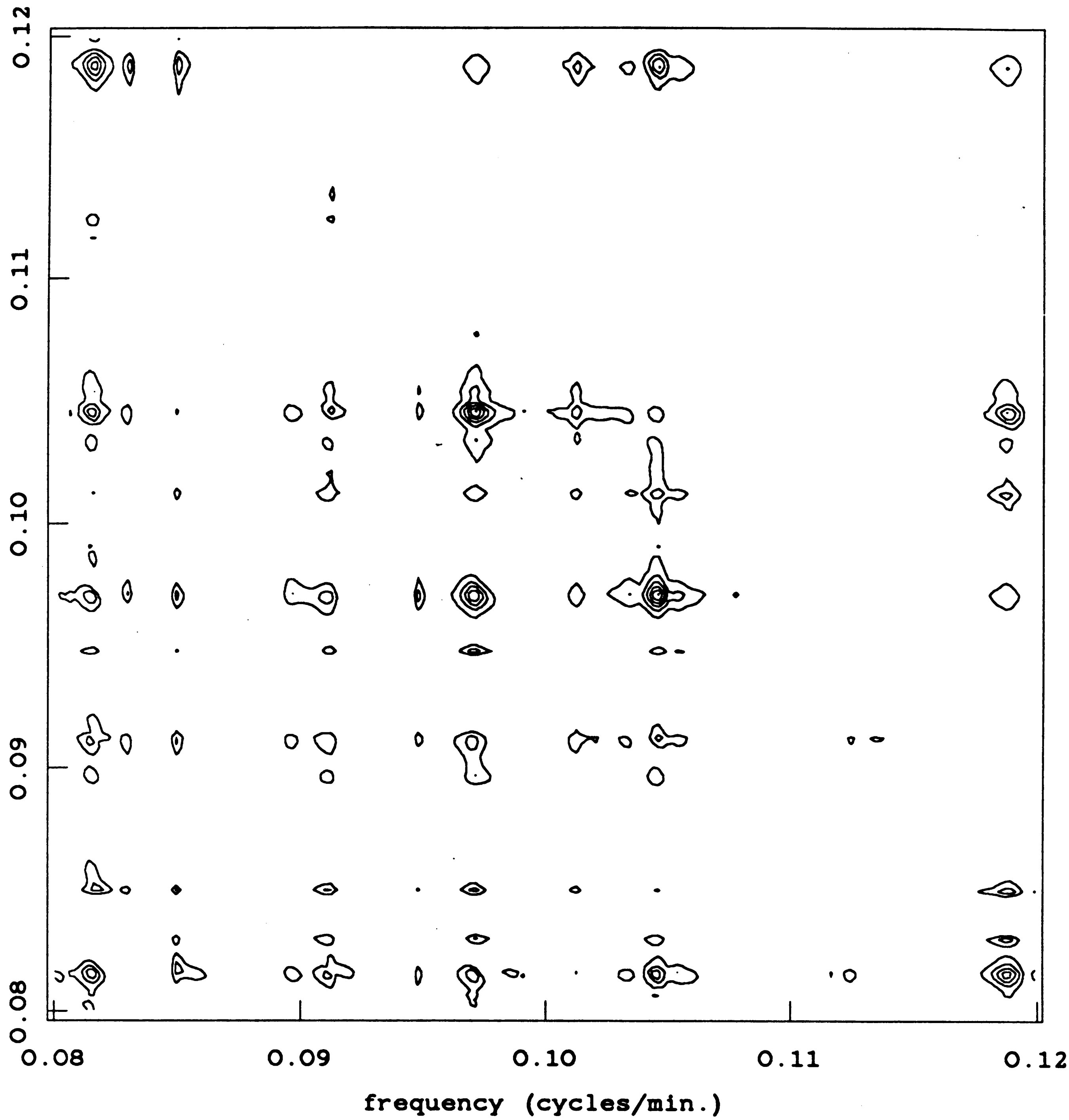

Fig. 5

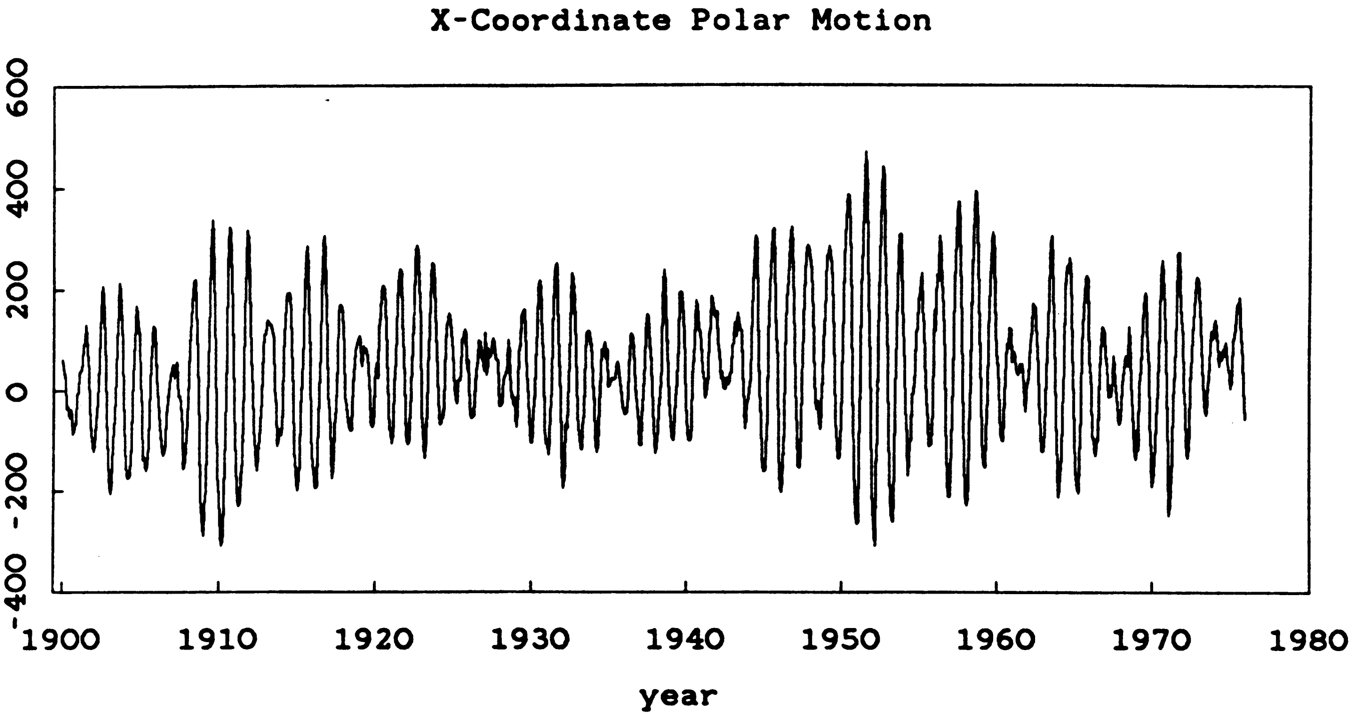
X-Coordinate Polar Motion
600
400
200
0
-200
-400
1900
1910
1920
1930
1940
1950
1960
1970
1980
year

Fig. 6

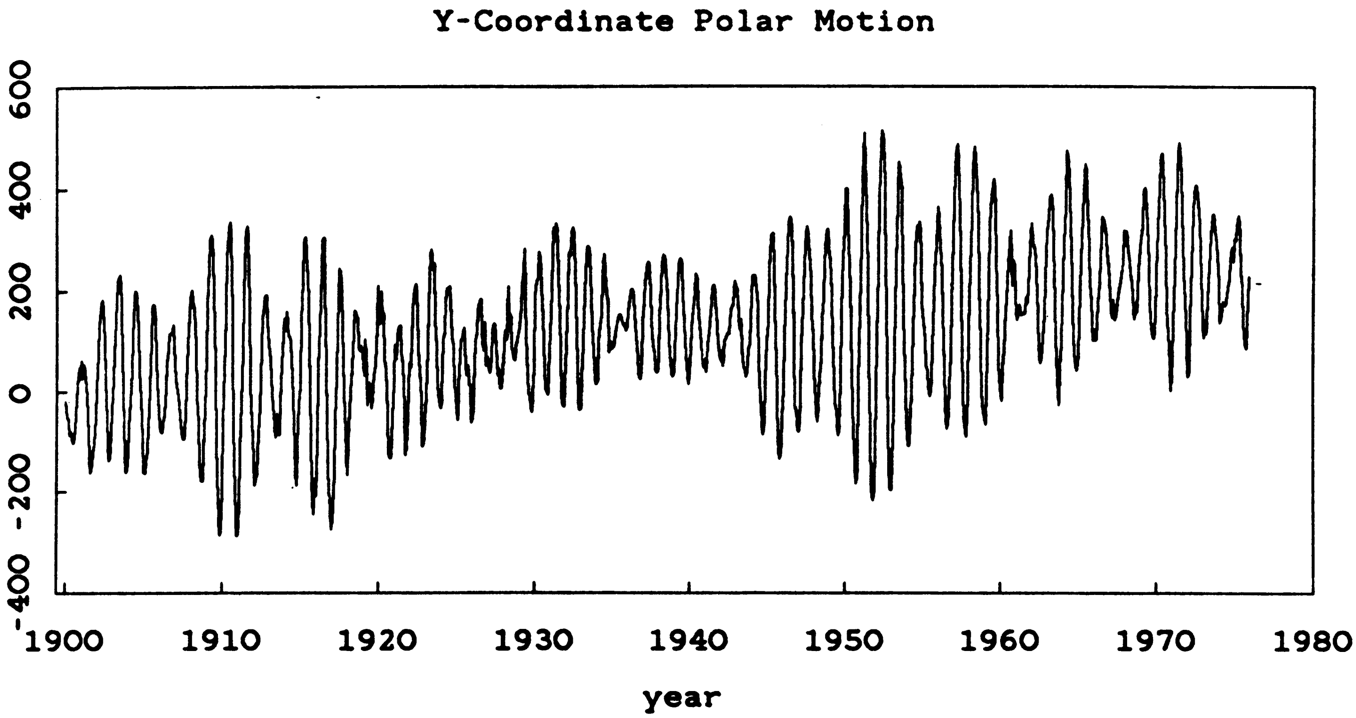
Y-Coordinate Polar Motion
600
400
200
0
-200
-400
1900
1910
1920
1930
1940
1950
1960
1970
1980
year

Fig. 7

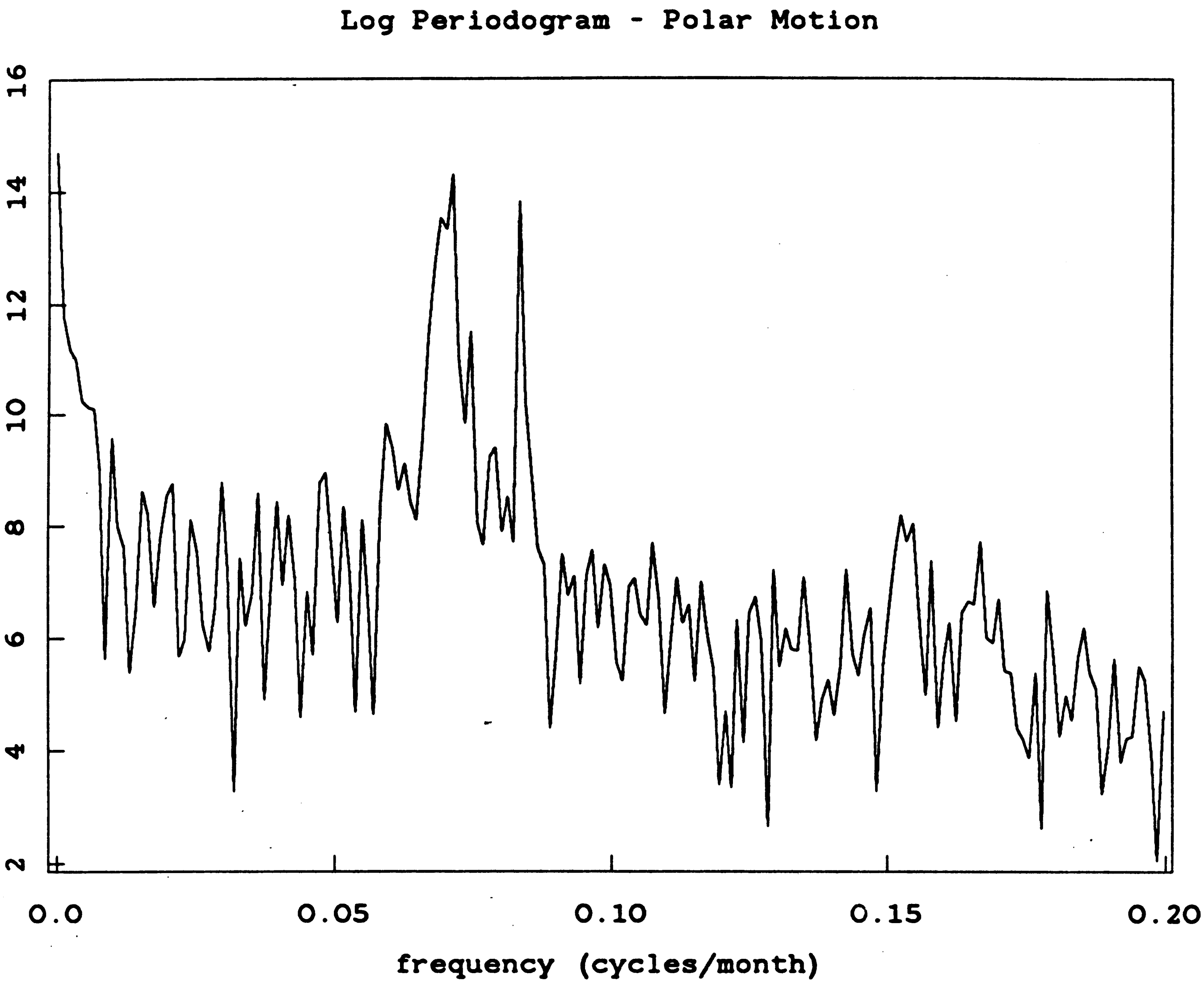

Log Periodogram - Polar Motion
2
4
6
8
10
12
14
16
0.0
0.05
0.10
0.15
0.20
frequency (cycles/month)

Fig. 8

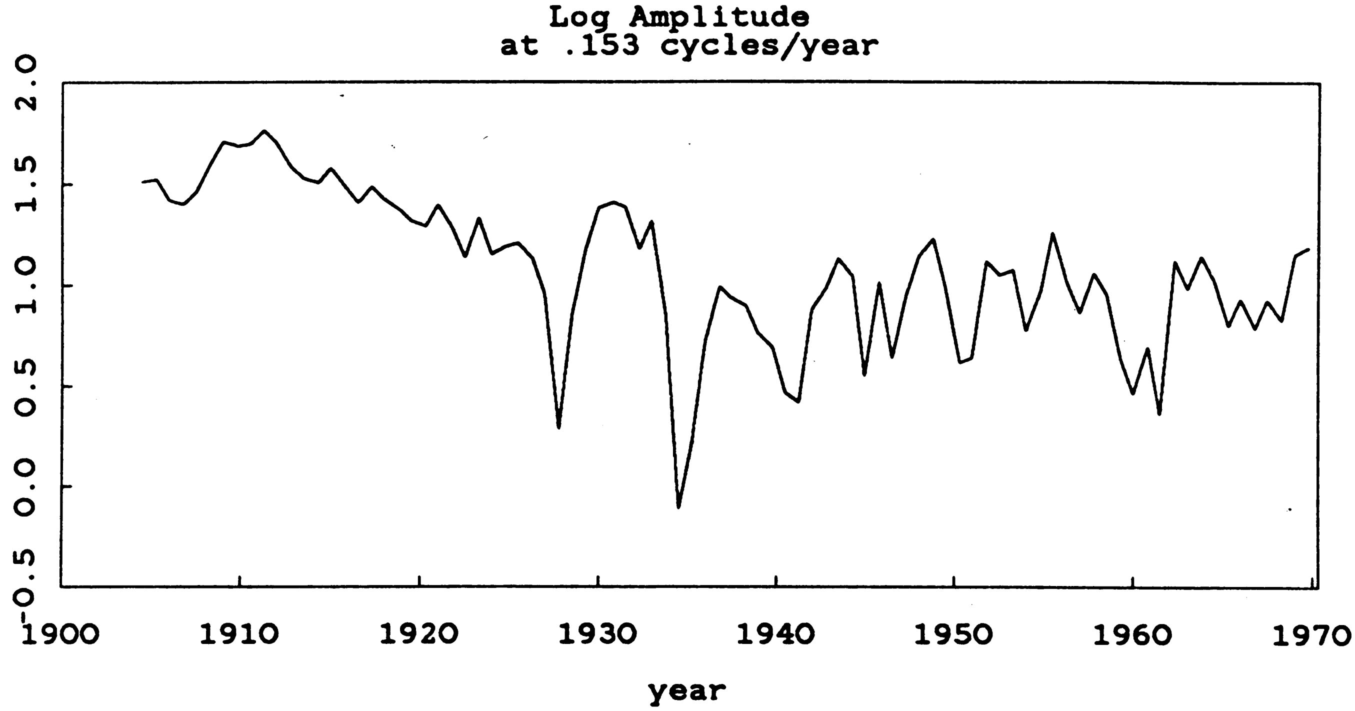
Log Amplitude
at .153 cycles/year
-0.5
0.0
0.5
1.0
1.5
2.0
1900
1910
1920
1930
1940
1950
1960
1970
year

Fig. 9

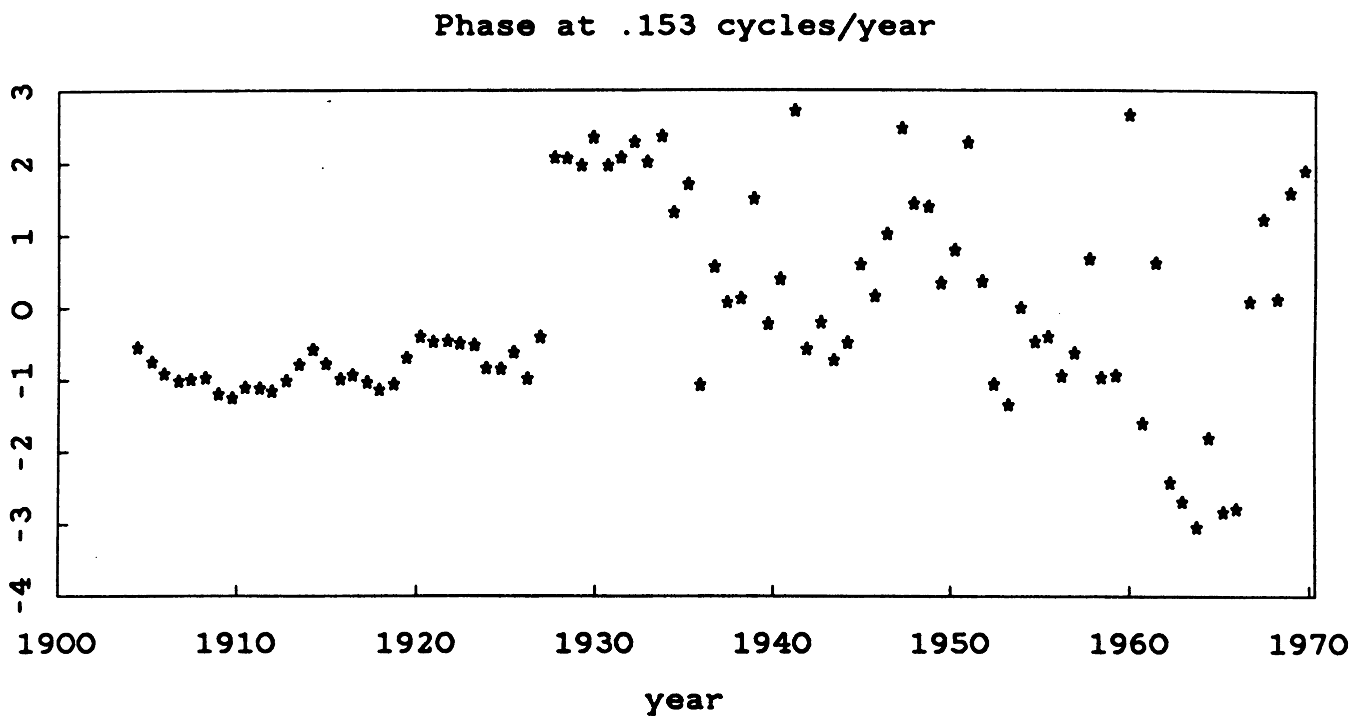
Phase at .153 cycles/year
3
2
1
0
-1
-2
-3
-4
1900
1910
1920
1930
1940
1950
1960
1970
year

Fig. 10